Prostate Cancer: MR Imaging–guided Galvanotherapy—Technical Development and First Clinical Results[1]

Thomas J. Vogl, MD
Heinz P. Mayer, MD
Stefan Zangos, MD
J. Bayne Selby, Jr, MD
Hanns Ackermann, MD
Florian B. Mayer, MD

Purpose: To prospectively evaluate the safety and effectiveness of magnetic resonance (MR) imaging–guided galvanotherapy in prostate cancer.

Materials and Methods: This prospective study was approved and authorized by the institutional review board, and patients gave informed consent. Forty-four men (mean age, 63.1 years) with histologically proved prostate cancer were treated with galvanotherapy. After transgluteal puncture of the prostate with local anesthesia, two MR imaging–compatible electrodes were positioned under MR imaging guidance in the periphery of the right and left lobes of the prostate so that they had direct tumor contact. The patients were treated three times in 1-week intervals, and direct current was applied to the localized cancer in the prostate gland with a total charge of 350 coulombs. Follow-up with laboratory testing (prostate-specific antigen [PSA] levels) and endorectal MR imaging with tumor volume measurement was performed 3, 6, and 12 months after the procedure. The Friedman test was used to compare tumor volumes and PSA levels across the four time points.

Results: All patients tolerated MR imaging–guided galvanotherapy well without any major side effects or complications. Six patients had some reversible difficulty with urination, and five reported temporary unilateral leg paresthesia. Tumor volume as determined with MR imaging decreased from a pretherapeutic median of 1.90 to 1.12 cm^3, which corresponded to a significant ($P < .01$) reduction of 41%. One patient (2%) had complete remission and 18 (41%) had partial remission at follow-up 12 months after therapy. Twenty-three patients (52%) were classified as having stable disease. Two patients (5%) had progressive disease. Median PSA levels decreased in the 12-month control period from 7.05 to 2.4 ng/mL (66%, $P < .01$).

Conclusion: MR imaging–guided galvanotherapy is a safe procedure and can result in local control of prostatic carcinoma, with a concomitant reduction in the PSA level.

Supplemental material: *http://radiology.rsnajnls.org/cgi/content/full/245/2/895/DC1*

[1] From the Department of Diagnostic and Interventional Radiology, University Hospital Frankfurt, Johann Wolfgang Goethe-University, Theodor-Stern Kai 7, D-60590 Frankfurt am Main, Germany (T.J.V., S.Z., F.B.M.); Institute of Minimal Invasive Tumor Therapy, Regensburg, Germany (H.P.M.); and Department of Radiology, Medical University of South Carolina, Charleston, SC (J.B.S., H.A.). From the 2005 RSNA Annual Meeting. Received September 20, 2006; revision requested November 9; revision received December 14; accepted January 22, 2007; final version accepted June 11. **Address correspondence to** T.J.V. (e-mail: *t.vogl@em.uni-frankfurt.de*).

By definition, galvanotherapy is a therapeutic method that makes use of the healing effects of direct electric current. During galvanotherapy, an electric current is applied to tumor tissue by means of at least two electrodes. Galvanotherapy employs several mechanisms to destroy targeted tumor cells. The most important mechanism is the pH value shift between the anode and the cathode. The ionic movement to the inversely charged electrode is accompanied by a pH value shift in the vicinity of the electrodes, with values ranging between 2.1 and 12.9 (1,2). The reasons for the pH shift near the anode are due to the electrolysis of $2H_2O$, which creates O_2, $4H^+$, and $4e^-$. The increase in the H^+ ions is the first reason. The second one is that H^+ then reacts with $4Cl^-$ to create 4HCl and an acidic pH. At the cathode, electrolysis of $2H_2O + 2e^- \leftrightarrow H_2 + 2OH^-$. OH^- reacts with Na^+ to create NaOH, leading to a basic pH. Thus, the vicinity of the anode becomes acidic owing to the higher concentration of protons, and the surrounding area of the cathode tissue becomes alkaline because of the higher concentration of OH^-. This derangement in pH value causes a denaturation of the cellular enzymes and, finally, cell death (2).

The movement of lymphocytes to the treated area after treatment has been evaluated by Chen et al (3); an increased reaction of the cellular immune functions of T and B lymphocytes and the nonspecific immune functions of the phagocytic system has also been observed (4). In additional experiments, immunocompetent and immunodeficient nude mice were treated with galvanotherapy, and much better treatment effects were detected in mice with intact immune systems (5). All these mechanisms result in a spherical area of necrosis around the electrodes with a diameter of up to 3 cm (6). Other advantages of this method in treating malignant tumors are the observed antimetastatic effect (7), as well as microne-crosis and the occlusion of local arteries and veins found in histologic specimens (8,9). In perfusion and oxygenation measurements of treated tumor tissue, Jarm et al (9) found significantly decreased values of both parameters. Limitations of galvanotherapy are tumor size (the cure rate decreases for tumors > 8 cm) and location (10). Lesions in the direct vicinity of major vessels or nerves must be treated very carefully because of the destructive effect of galvanotherapy.

Magnetic resonance (MR) imaging–guided galvanotherapy focuses on tumor cells because of their electrical properties, on the basis of the fact that the electrical resistance of cancer cells is lower than that of healthy cells (11–13). Accordingly, the current preferentially travels through the low-resistance tumor rather than through the relatively high-resistance normal tissue. Cells are destroyed without any concomitant thermal reaction (14,15).

The concept of MR imaging–guided galvanotherapy of the prostate is based on percutaneous access, with the goal of preserving the potency and continence of the patients. For electrophysiologic reasons, MR compatible electrodes are positioned, as described by Zangos et al (16), with direct tumor contact. The purpose of our study was to prospectively evaluate the safety and effectiveness of MR imaging–guided galvanotherapy in prostate cancer.

Advances in Knowledge

- Local tumor control and a decrease in tumor size resulted from MR imaging–guided galvanotherapy.
- MR imaging–guided galvanotherapy caused a decrease in the prostate-specific antigen level (from 7.05 to 2.4 ng/mL).

Implication for Patient Care

- MR imaging–guided galvanotherapy appears to be a safe and effective way to treat prostate cancer, although our results are preliminary.

Materials and Methods

Patients and Follow-up

This prospective study was approved and the investigation was authorized by the institutional review board of University Hospital Frankfurt. Informed consent was obtained from all patients included in the study. A total of 44 men (mean age, 63.1 years; range, 49–78 years) were evaluated from February 2005 through August 2006. Disease was staged with 1.5-T MR imaging and bone scanning as T1N0M0 ($n = 17$), T2N0M0 ($n = 22$), and T3N0M0 ($n = 5$), and all men who met the criteria and agreed to participate in our study were included. Pretherapy diagnostic tests included a 1.5-T MR imaging examination (Sonata; Siemens, Erlangen, Germany) to localize the lesion; histologic examination (proof) of the prostate cancer after biopsy; and laboratory testing, including the determination of prostate-specific antigen (PSA) levels. Oncologic staging also included radiography of the chest and bone scanning. Exclusion criteria were as follows: patients who had undergone any treatment of the prostate cancer before galvanotherapy; patients who had metastases to the lung, bones, or lymph nodes at presentation; and patients in whom MR imaging could not be performed (eg, patients with pacemakers).

When patients with elevated PSA levels but without biopsy-proved cancer were enrolled, a biopsy was then per-

Published online
10.1148/radiol.2453061623

Radiology 2007; 245:895–902

Abbreviation:
PSA = prostate-specific antigen

Author contributions:
Guarantor of integrity of entire study, T.J.V.; study concepts/study design or data acquisition or data analysis/interpretation, all authors; manuscript drafting or manuscript revision for important intellectual content, all authors; manuscript final version approval, all authors; literature research, T.J.V., F.B.M.; clinical studies, T.J.V., H.P.M., S.Z., J.B.S., F.B.M.; statistical analysis, H.A.; and manuscript editing, T.J.V., J.B.S.

Authors stated no financial relationship to disclose.

formed to determine whether the patient had prostate cancer. The interval between biopsy and the first treatment session was at least 1 week to allow the patients to recover sufficiently. Patients who had positive biopsy results at presentation could undergo diagnostic imaging and the first treatment in 1 day. Galvanotherapy was started within 14 days after MR imaging and biopsy. The patients were treated on an outpatient basis for a total of three sessions in 1-week intervals.

Galvanotherapy Procedure

Prior to biopsy and galvanotherapy, all patients underwent MR imaging with an endorectal coil and a standard imaging protocol consisting of transverse (repetition time msec/echo time msec, 2400/109) (Fig 1a), sagittal (2500/109), and coronal (4160/106) fast spin-echo sequences with section thicknesses of 3.0, 4.0, and 3.0 mm and intersection gaps of 0.3, 0.4, and 0.3 mm, respectively (17).

For biopsy, access to the prostate was gained with an MR imaging–guided needle puncture by using a 0.2-T open MR imaging unit (Magnetom Concerto; Siemens). Data sets were acquired with 180/13, an intersection gap of 0.6 mm, and a section thickness of 8 mm. Advantages of this procedure were the real-time imaging option and lateral access to the patients' back sides for the biopsy. With the indoor monitor we were able to stay directly beside the patient during the entire procedure. The disadvantage of 0.2-T open MR imaging is the low spatial resolution compared with that of 1.5-T imaging. Before the first galvanotherapy treatment, every patient underwent biopsy once in accordance with the procedure defined by Zangos et al (16).

One week after biopsy, the first of three galvanotherapy treatments (performed weekly) was performed while the patients were in mild sedation after administration of 10 mg tramadol HCl (Tramal; Grünenthal, Aachen, Germany) and 10 mg diazepam (Valium; ratiopharm, Ulm, Germany). Two MR imaging–compatible electrodes were introduced with 20 mL of local anesthesia (Lidocain 1%; AstraZeneca, Wedel, Germany) for each puncture site. We adopted the procedure used by Zangos et al (16) to perform biopsy; however, we did not actually perform biopsy but instead placed the electrodes by using a posterior transgluteal approach (Fig 1b). The patient was placed in the prone position to allow real-time MR imaging–guided puncture and to facilitate access by the physician. After the path for the procedure was chosen, the point of insertion was marked by taping it with an MR imaging–visible marker or by using real-time imaging together with a finger as an external marker. The receiver was a flexible standard multipurpose coil (Siemens) with a diameter of 45 cm. The coil was positioned at the level of the greater trochanter.

Constant monitoring and evaluation of the path of the puncture instruments, as well as additional imaging management, was performed with a standard in-room workstation (Siemens). The previously sampled MR images were employed for planning the puncture path. The puncture site was prepared, draped, and sterilized, and local anesthesia was administered. Owing to the fact that it is difficult to delineate the lesions, we found a way to reconstruct their positions on the basis of the 1.5-T images. We used the ventrodorsal di-

Figure 1

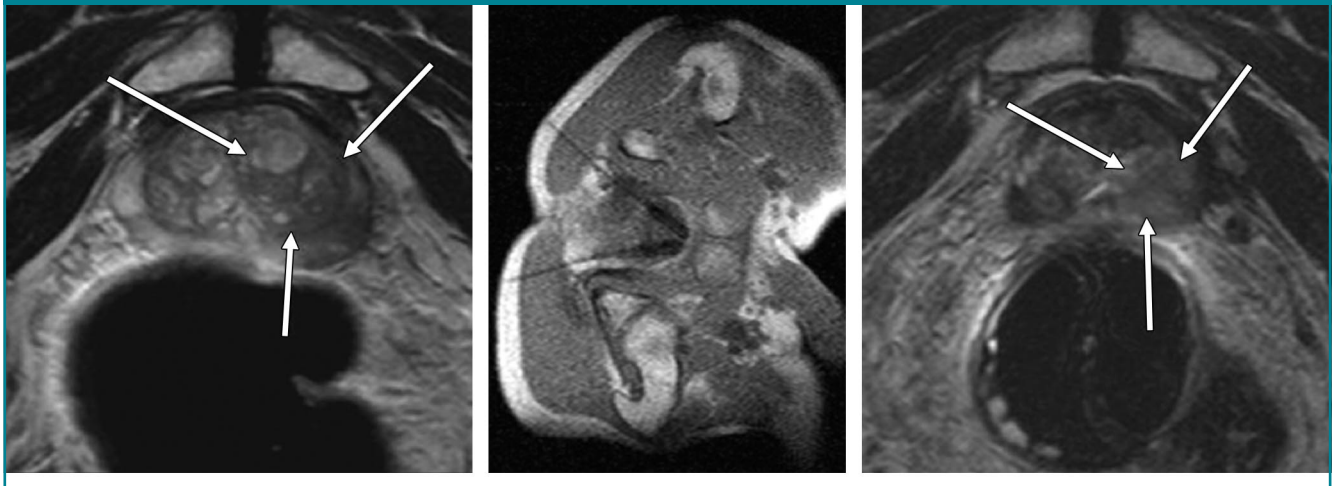

a. b. c.

Figure 1: Transverse MR images in 58-year-old patient with T2N0M0 prostate cancer in left peripheral zone with complete remission at 12-month follow-up. All images except **b** (obtained with a 0.2-T open MR imaging unit) were obtained at 1.5 T. **(a)** Pretherapy endorectal intermediate-weighted image (2500/46) shows nodular lesion with decreased signal intensity (arrows) and capsular infiltration without extracapsular spread. **(b)** Gradient-echo T2-weighted fast low-angle shot image (180/13) obtained during galvanotherapy documents access of MR imaging–compatible electrodes and their position in periphery of prostate gland. **(c)** Intermediate-weighted image (2500/46) obtained 12 months after therapy. Image shows new homogeneity of the malignant area (arrows) in left posterior lobe. The PSA level decreased from 5.7 to 2.1 ng/mL during the 12 months from the intervention to the final examination. The imaging findings were classified as showing partial remission.

ameter of the femoral head to transfer the position located in the 1.5-T diagnostic study to the 0.2-T open MR imaging study, and we detected these typical landmarks and inserted the MR imaging–compatible puncture needle (Somatex, Teltow, Germany) to ascertain the correct height of the prostate. Next, the inner stylet of the needle was removed, and the MR imaging–compatible galvanoelectrode was introduced through the cannula. The hollow needle was pulled back to expose the galvanotherapy electrode. The 0.5 × 200-mm MR–imaging compatible electrodes (Galvaneedle, Regensburg, Germany), which were made of titanium-nickel alloys and coated with platinum at the tip, were introduced.

The two electrodes were isolated between the two conductive ends "A" and "B." The "A" ends were connected to the direct current source, and the "B" ends were located in the prostate. The conductive tips of the "B" ends had the same length as the maximum dorsoventral tumor diameter. The open 0.2-T MR imaging unit with a vertical field axis was used to guide the needles for the puncture because it enabled wide lateral access to the patient. From an electrophysiologic point of view, it was very important to place the "B" ends on either side of the tumor lesion. If the tumor was located in the periphery of the prostate gland, the negative electrode was placed in the periphery of the lesion and the anode was placed in the center of the lesion. This takes advantage of the more destructive effect of the positive electrode (18–21). If the lesion was in the center of the prostate, both "B" ends were placed in the periphery of the lesion. Because of this "B"-end configuration, the current was focused on the lesion. After the electrodes were secured at the skin to avoid any changes of position, they could be connected to the direct current applicator. If MR imaging and biopsy findings did not match, we treated the histologically verified area and changed the electrode position from treatment to treatment around this area. All three galvanotherapy treatments were performed by two physicians (T.J.V., H.P.M.).

The position of the electrodes in the outer margin of the prostate was visualized with MR imaging sequences in two planes (transverse and coronal). Direct current was applied by using a medical apparatus (Galvaionic 75/32; Galvamedix, Regensburg, Germany). This apparatus is a microprocessor voltage supplier-regulator that is capable of providing direct current. To ensure a constant current, the resistance of the tumor was measured, and the voltage was regulated depending on the varying resistance of the tumor. At the beginning of the treatment, the electrical resistance was high. Accordingly, a high voltage for the current was needed. Patients reported that they experienced pain at the beginning of galvanotherapy as the current was increased. However, pain regularly abated after 5–10 minutes at this increased current level. After 10–15 minutes, the electrical resistance decreased from 600–800 Ω to 200–500 Ω. The varying resistance between 600 and 800 Ω depends on the distance between the electrodes. The total load applied is dependent on the total volume of the tumor. One hundred coulombs (C) per cubic centimeter have to be applied (22–25). The voltage range was between 5 and 10 V, while the current values were between 10 and 30 mA. The current was adapted to the patient's individual pain threshold.

Depending on the maximum achievable values, the patients received between 80 and 150 C in each treatment session, which lasted for a maximum of 3 hours. The treatment was limited to a maximum charge of 150 C because of the risk of increased swelling of the prostate gland should the application exceed this mark. The total charge that was regularly applied during the treatment session was 350 C. When the projected charge was reached, the current was slowly lowered to zero. If the current was decreased too quickly, patients often reported pain, as described below. To make sure that the complete area of suspicion was treated, we changed the anodic electrode position from cranial to caudal from one treatment to the next. Thus, the whole lobe was treated as well. After treatment, the electrodes were removed from the prostate gland, and a dressing was applied to the puncture site. Immediately after removal of the electrodes, the patients were instructed to lie in a supine position on the incisions to prevent intramuscular bleeding. We did not administer any prophylactic antibiotics. The entire method, including follow-up computed tomography (CT), demanded constant supervision of the patients by a physician to observe the treatment and address possible side effects. All procedures were performed by two physicians working together (T.J.V. and F.B.M.).

Patients were clinically observed for at least 2 hours so that we could monitor any side effects such as temporary paresthesia in a leg or bleeding. Pain was assessed by using a standardized assessment scale from 0 to 10, with a score of 10 indicating the most severe pain. After 2 hours of observation, the patients underwent unenhanced low-dose CT, which is more sensitive for excluding complications such as rectal, local, and pelvic bleeding or free air caused by perforation of the bowel. In physical examinations, side effects such as paresthesia, hematuria, urination problems, and reduced physical strength were evaluated. All patients went home on the day of treatment and were given an emergency cellular phone number. Patients were then contacted and interviewed about any side effects or complications and to check progress at 3, 6, and 12 months after the last therapy. Imaging during the current application could not be performed for physical reasons—that is, because a direct current depends on a polarized field between galvanoelectrodes, leading to an orientation of the protons in the field direction. The magnetic field is not strong enough to compensate for this effect; therefore, no image can be received.

Follow-up included MR imaging, PSA testing, and patient interviews. The follow-up results were then evaluated and compared with the findings before galvanotherapy. All images were evaluated by two readers (T.J.V. and S.Z., who had more than 10 and 5 years of experience, respectively, in evaluation of MR images of the prostate), who worked

together in consensus. The evaluation consisted of measurement of the lesions and lymph nodes and a comparison of these findings with pretherapy MR imaging findings. For the volume measurement, we used transverse and coronal images from the 1.5-T MR imaging examination and assessed the maximum diameter in all three dimensions. Therefore, the MR imaging measurement tool was used. To calculate the volume from the three diameters (D_1, D_2, and D_3), we used the following formula: $(D_1 \cdot D_2 \cdot D_3) \cdot 0.523$. The PSA values were also obtained before treatment and 3, 6, and 12 months thereafter. We recommended conventional radiography of the chest and bone scintigraphy on an annual basis to exclude development of metastases.

Statistical Analysis

The follow-up MR imaging results and PSA levels were compared with the results of the pretherapy diagnostic 1.5-T MR imaging examination and the PSA levels before galvanotherapy. Patients were admitted with histologically proved prostate carcinoma but without Gleason scores; accordingly, we cannot provide Gleason score data. Furthermore, the number of samples in the patients who had already undergone biopsy varied. The patients who underwent biopsy at our institution underwent sextant biopsy. So that we could judge the effectiveness of this treatment, the following criteria were used: Partial remission was defined as a 30% reduction in the total size of the tumor, with no new lesions. Stable disease was defined as a less than 30% reduction in the size of the tumor, with the development of no new lesions. Progressive disease was defined as an increase in the measurable intra- or extraprostatic tissue or the growth of new tissue lesion. Complete remission was defined as a 100% decrease in tumor size.

No second biopsies were performed during or after the treatments because our institutional review board decided against repeat biopsy because of the possible risk of infection in the treated tumor tissue.

PSA values and tumor size pretherapy and at 3, 6, and 12 months after therapy were compared by using the Friedman test; when differences were significant ($P < .05$), we performed pairwise comparisons by using the Wilcoxon signed rank test. We used statistical software (BiAS for Windows, version 8.2.8).

Results

MR Imaging Findings

Median tumor size, as measured at MR imaging, decreased from 1.90 cm^3 before therapy to 1.12 cm^3 after therapy; this corresponded with a significant reduction ($P < .01$) of 41%. Of the 44 patients who underwent examination 3 months after therapy, eight (18%) had partial remission and volume reduction of more than 30% at MR imaging. Thirty-four patients (77%) were classified as having stable disease. Two patients (5%) showed disease progression, with an increase in tumor size of at least 30%.

The 6-month follow-up produced the following results: 17 men (39%) showed a partial remission of the lesion. Tumor size was reduced by up to 30% in 25 patients (57%), and in two patients (5%), the lesion increased in volume by more than 30% compared with the volume on the pretherapeutic images.

At follow-up MR imaging 12 months after therapy, one man (2%) demonstrated complete remission (Fig 1), 18 men (41%) showed partial remission of the neoplastic area (Fig 2), and 23 patients (52%) showed stable disease (Fig 3). Two patients (5%) again showed progressive disease (Fig 4). Pretherapy MR images, electrode positioning in all three treatments, and the follow-up 1.5-T MR images were reevaluated in these two patients, but no different parameters or factors could be found. All patients in the stable disease category had decreasing tumor volumes. There were no statistically significant differences between the results with treated T1, T2, or T3 tumors ($P = .13$).

According to our experience, there was no edematous change in tumor or normal tissue, and no lymph nodes or bone metastases were detected in any patients.

PSA Values

The initial pretreatment PSA values ranged from 0.44 to 96.6 ng/mL, with a median of 7.05 ng/mL (Table E1, *http://radiology.rsnajnls.org/cgi/content/full/245/2/895/DC1*). At 3 months, a 26% decrease in the median value, to 5.25 ng/mL, was observed. At 6

Figure 2

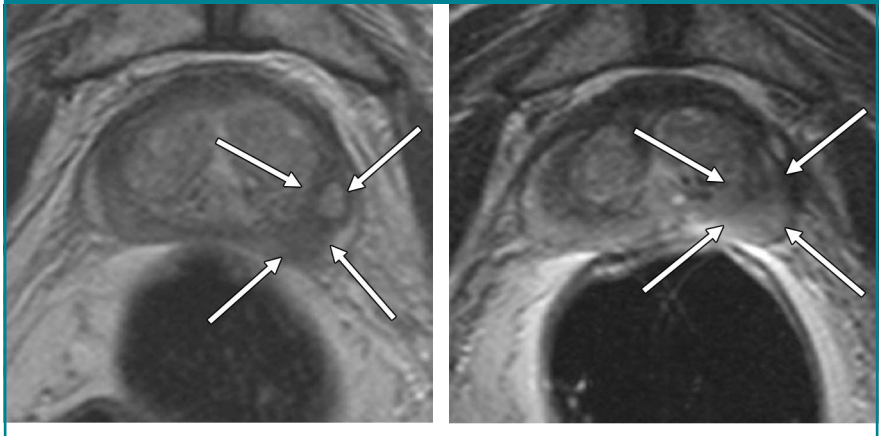

a. b.

Figure 2: Transverse intermediate-weighted MR images (2500/46) in 63-year-old patient with T2N0M0 prostate cancer in left lobe. Partial remission was achieved. **(a)** Pretherapy image shows the tumor (arrows) in periphery of left lobe of prostate. The signal intensity decrease marks the lesion with capsular infiltration but no extracapsular spread. **(b)** Image at 12-month follow-up shows partial remission, with an increase in the signal intensity of the left peripheral zone and a full decrease in volume of the tumor (arrows).

months, the median PSA had decreased to 4.05 ng/mL, a total decrease of 43%. The 12-month PSA values ranged from 0.02 to 55 ng/mL, with a 66% decrease in the median value, from 7.05 to 2.4 ng/mL.

If the values at the pretherapeutic and the 12-month posttherapeutic evaluations were compared by using the Friedman test and the results were significant ($P < .05$), the Wilcoxon signed rank test was used. Our findings show that we achieved a significant decrease in PSA level, with $P < .01$. The pretherapeutic PSA values were also significantly different from the 3-month posttherapeutic PSA values, with $P < .004$. The 6-month set of posttherapy PSA values was also significantly ($P < .01$) different from pretherapeutic PSA values (Fig 5).

Figure 3

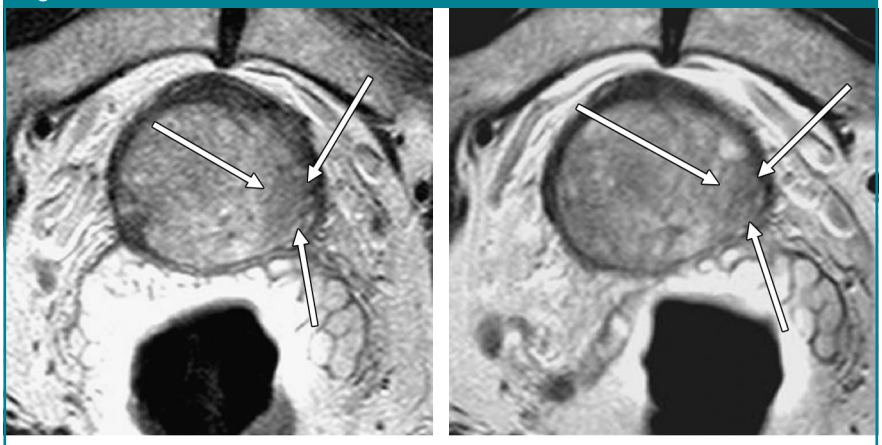

a. b.

Figure 3: Transverse intermediate-weighted MR images in 75-year-old patient with T2N0M0 prostate cancer in peripheral zone of left lobe show stable disease at follow-up. **(a)** Endorectal image (5280.0/109.0) shows the lesion (arrows) in left posterior lobe of prostate, without infiltration of the capsule. **(b)** Image at 12-month follow-up shows finding of stable disease (arrows) after three MR imaging–guided galvanotherapy treatments in left posterior lobe. There is increase in the signal intensity of the tumor and homogenization of the entire lesion.

Figure 4

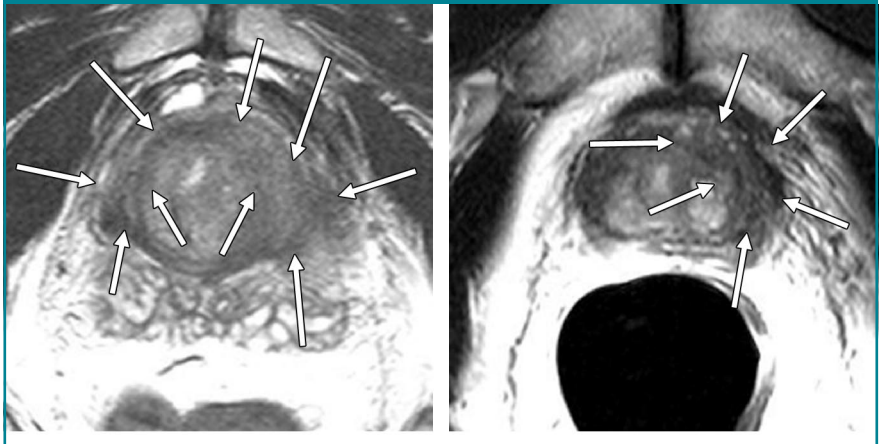

a. b.

Figure 4: Transverse MR images in 50-year-old patient with bilateral T3N0M0 prostate cancer with capsular infiltration and progressive disease. **(a)** Pretherapy image shows bilateral tumor, including extensive *U*-shaped infiltration (arrows) of the right and left sides, as well as the ventral part, of the capsule. Pretherapy PSA value was 96.6 ng/mL. **(b)** Image obtained 12 months after therapy shows progression in left lobe (arrows) and stable disease in right lobe.

Side Effects and Complications

The application of direct current resulted in moderate local pain, which was tolerated without the use of narcotics. When the direct current was increased, patients often reported a blunt or pushing feeling in the punctured region of the prostate, but never asked for further pain-reducing medication. The median of the pain scale score during the entire time of treatment was 3. The 1st and 3rd quartiles were between 2 and 4. During the 3 days after therapy, the median pain score was 1. The most common side effects were temporary difficulties with urination ($n = 6$) and temporary hematuria ($n = 6$). In all 12 patients who experienced side effects, signs and symptoms resolved within 24 hours without therapeutic intervention. Five patients noticed a reduction in their physical strength (resulting in minor impairment of their quality of life during the next 2–3 days), and five patients had a temporary paresthetic feeling in one leg caused by the local diffusion of the local anesthesia. In these patients, no treatment was necessary, and the symptoms had completely resolved by the time the patients left the clinic. In one case, a patient developed prostatitis, which was treated successfully with antibiotics, and full recovery was achieved after 4 weeks. Furthermore, posttherapy CT results excluded any rectal perforation or local or pelvic bleeding. The follow-up interview with the patients showed that there was no case of impotence or incontinence or other long-term side effect in our study population during the period of observation.

Discussion

Established therapies for prostate cancer include radical prostatectomy, radi-

Figure 5

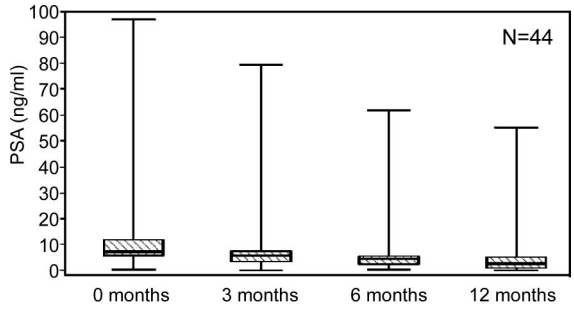

Figure 5: Bar graph shows course of PSA levels during posttherapy period compared with pretherapeutic values. Median PSA values showed a decrease from 7.1 to 5.25 ng/mL (26%) after 3 months. Median value at second follow-up (after 6 months) was 4.05 ng/mL (a decrease of 43%). The last PSA test showed a decrease of 66% to an absolute median value of 2.4 ng/mL. When the first and the last values were compared by using the Wilcoxon signed-rank test, a highly significant value, $P < .01$, was found. Error bars show standard deviations.

ation, and hormonal therapy. Despite the benefits of these therapies, there are disadvantages that present the patient with major physical problems. In addition to acute side effects of surgery, including bleeding, infection, and perforation of neighboring organs and nerves, unintentional long-term effects after treatment such as impotence or incontinence are very important quality of life issues for patients. Furthermore, general anesthesia during surgery involves risks. Data on the side effects of radical prostatectomy showed that 30%–80% of the patients had erectile dysfunction (26,27). Men subjected to external radiation therapy have rates of erectile dysfunction of 33%–51% (27,28). The hormonal option often leads to gynecomastia, which men find psychologically difficult to deal with. Faced with these disturbing side effects of traditional treatments for men with prostate carcinoma, new therapy options with fewer side effects are being evaluated.

MR imaging–guided galvanotherapy represents a promising addition to the armamentarium to treat prostate cancer. The direct electric effect causes cell death—preferentially to tumor cells, which are more susceptible (as described at the beginning of this article). Results with galvanotherapy indicate that it involves a large number of mechanisms attacking the cancerous tissue, with different results. Because of this variety, there is variable influence on the death, proliferation, and oxygenation of cells; the development of metastasis; the positive effect on the immune system; and the development of non-pH-value–shifted necrosis in the voltage field.

The most important drawback of this treatment technique is when the tumor is large (>8 cm), which diminishes long-term outcome in almost every kind of malignancy. Other limitations are the formation of metastases in distant tissues before galvanotherapy and the possible destruction of major vessels and nerves located in the area of spreading necrosis (10).

Data from our initial patients indicate that MR imaging–guided galvanotherapy appears to be a safe and effective way to treat prostate cancer. In the 44 patients we treated in our study, we observed only two with progressive disease, pointing toward successful treatment with local tumor control in 95% of all men, without any development of impotence or incontinence. A great fear for patients with prostate cancer is the appearance of metastases in the lymph nodes or bones. No patient in our study developed metastases during the time of observation.

As our study results show, MR imaging–guided galvanotherapy is a viable option for treating prostate carcinoma. None of the patients treated had any signs of organ perforation or rectal bleeding, and no hematuria was observed after 24 hours. The few side effects of MR imaging–guided galvanotherapy that were reported disappeared within 24 hours, and no further interventions were required. The potential risk of perforation of the bladder or the intestine is minimized by using MR imaging guidance to direct the puncture, and perforation did not occur in our study group. Limitations of our study were the small number of patients, the lack of an ideal reference standard such as whole-mount prostatectomy, and no long-term data for longer than 12 months regarding the outcome of disease for both local tumor treatment rate and development of distant metastases. Furthermore, the T2-weighted diagnostic and follow-up MR images, as compared with biopsy of the treated tumor area, were suboptimal for assessing prostate lesions to evaluate the local effects of galvanotherapy. As already stated, our institutional review board would not approve such biopsies.

In summary, encouraging but preliminary results were achieved after three sessions of MR imaging–guided galvanotherapy, with a minimum of long-term side effects and a concomitant reduction in PSA values and imaging findings. Additional studies are needed for evaluation of this treatment technique.

References

1. Li K, Xin Y, Gu Y, Xu B, Fan D, Ni B. Effects of direct current on dog liver: possible mechanisms for tumor electrochemical treatment. Bioelectromagnetics 1997;18:2–7.

2. Yen Y, Li J, Zhou B, Rojas F, Yu J, Chou C. Electrochemical treatment of human KB cells in vitro. Bioelectromagnetics 1999;20:34–41.

3. Chen B, Xie Z, Zhu F. Experimental study on electrochemical treatment of cancer in mice. Eur J Surg Suppl 1994;574:75–77.

4. Gong HY, Liu GZ. Effect of electrochemical therapy on immune functions of normal and

tumour-bearing mice. Eur J Surg Suppl 1994;574:73–74.

5. Miklavcic D, An D, Belehradek J, Mir L. Host's immune response in electrotherapy of murine tumors by direct current. Eur Cytokine Netw 1997;8:275–279.
6. Xin Y, Xue F, Ge B, Zhao F, Shi B, Zhang W. Electrochemical treatment of lung cancer. Bioelectromagnetics 1997;18:8–13.
7. Orlowski S, An D, Belehradek J, Mir L. Antimetastatic effects of electrochemotherapy and of histoincompatible interleukin-2-secreting cells in the murine Lewis lung tumor. Anticancer Drugs 1998;9:551–556.
8. Miklavcic D, Jarm T, Cemazar M, et al. Tumor treatment by direct electric current: tumor perfusion changes. Bioelectrochem Bioenerg 1997;43:253–256.
9. Jarm T, Cemazar M, Steinberg F, Streffer C, Sersa G, Miklavcic D. Perturbation of blood flow as a mechanism of anti-tumour action of direct current electrotherapy. Physiol Meas 2003;24:75–90.
10. Nilsson E, von EH, Berendson J, et al. Electrochemical treatment of tumours. Bioelectrochemistry 2000;51:1–11.
11. Haemmerich D, Staelin S, Tsai J, Tungjitkusolmun S, Mahvi D, Webster J. In vivo electrical conductivity of hepatic tumours. Physiol Meas 2003;24:251–260.
12. Cameron IL, Smith NK, Pool TB, Sparks RL. Intracellular concentration of sodium and other elements as related to mitogenesis and oncogenesis in vivo. Cancer Res 1980;40:1493–1500.
13. Smith NR, Sparks RL, Pool TB, Cameron IL. Differences in the intracellular concentration of elements in normal and cancerous liver cells as determined by X-ray microanalysis. Cancer Res 1978;38:1952–1959.
14. Miklavcic D, Sersa G, Kryzanowski M, et al. Tumor treatment by direct electric current: tumor temperature and pH, electrode material and configuration. Bioelectrochem Bioenerg 1993;30:209–220.
15. Baxter PS, Wemyss-Holden SA, Dennison AR, Maddern GJ. Electrochemically induced hepatic necrosis: the next step forward in patients with unresectable liver tumours? Aust N Z J Surg 1998;68:637–640.
16. Zangos S, Eichler K, Engelmann K, et al. MR-guided transgluteal biopsies with an open low-field system in patients with clinically suspected prostate cancer: technique and preliminary results. Eur Radiol 2005;15(1):174–182.
17. Wetter A, Hubner F, Lehnert T, et al. Three-dimensional 1H-magnetic resonance spectroscopy of the prostate in clinical practice: technique and results in patients with elevated prostate-specific antigen and negative or no previous prostate biopsies. Eur Radiol 2005;15:645–652.
18. Turler A, Schafer H, Schafer N, et al. Pilot study of effectiveness of electrotherapy in the experimental liver metastasis model [in German]. Langenbecks Arch Chir Suppl Kongressbd 1998;115(suppl I):611–614.
19. Maintz D, Fischbach R, Schafer N, Schafer H, Gossmann A, Kugel H. Results of electrochemical therapy of colorectal liver metastases in rats followed up by MRI. Invest Radiol 2000;35:289–294.
20. Griffin DT, Dodd NJ, Moore JV, Pullan BR, Taylor TV. The effects of low-level direct current therapy on a preclinical mammary carcinoma: tumour regression and systemic biochemical sequelae. Br J Cancer 1994;69:875–878.
21. Robertson GS, Wemyss-Holden SA, Dennison AR, Hall PM, Baxter P, Maddern GJ. Experimental study of electrolysis-induced hepatic necrosis. Br J Surg 1998;85:1212–1216.
22. Samuelsson L, Jonsson L. Electrolyte destruction of lung tissue: electrochemical aspects. Acta Radiol Diagn (Stockh) 1980;21:711–714.
23. Ren RL, Vora N, Yang F, et al. Variations of dose and electrode spacing for rat breast cancer electrochemical treatment. Bioelectromagnetics 2001;22:205–211.
24. Xin YL. Advances in the treatment of malignant tumours by electrochemical therapy (ECT). Eur J Surg Suppl 1994;574:31–35.
25. Turler A, Schaefer H, Schaefer N, et al. Experimental low-level direct current therapy in liver metastases: influence of polarity and current dose. Bioelectromagnetics 2000;21:395–401.
26. Steineck G, Helgesen F, Adolfsson J, et al. Quality of life after radical prostatectomy or watchful waiting. N Engl J Med 2002;347:790–796.
27. Vale J. Erectile dysfunction following radical therapy for prostate cancer. Radiother Oncol 2000;57:301–305.
28. Sanchez-Ortiz RF, Broderick GA, Rovner ES, Wein AJ, Whittington R, Malkowicz SB. Erectile function and quality of life after interstitial radiation therapy for prostate cancer. Int J Impot Res 2000;12(suppl 3):S18–S24.

Radiology 2007

This is your reprint order form or pro forma invoice

(Please keep a copy of this document for your records.)

Reprint order forms and purchase orders or prepayments must be received 72 hours after receipt of form either by mail or by fax at 410-820-9765. It is the policy of Cadmus Reprints to issue one invoice per order. **Please print clearly**.

Author Name _____
Title of Article _____
Issue of Journal_____ Reprint # _____ Publication Date _____
Number of Pages_____ KB # _____ Symbol Radiology
Color in Article? Yes / No (Please Circle)

Please include the journal name and reprint number or manuscript number on your purchase order or other correspondence.

Order and Shipping Information

Reprint Costs (Please see page 2 of 2 for reprint costs/fees.)

_____ Number of reprints ordered $_____
_____ Number of color reprints ordered $_____
_____ Number of covers ordered $_____
Subtotal $_____
Taxes $_____

(*Add appropriate sales tax for Virginia, Maryland, Pennsylvania, and the District of Columbia or Canadian GST to the reprints if your order is to be shipped to these locations*.)

First address included, add $32 for each additional shipping address $_____

TOTAL $_____

Shipping Address (cannot ship to a P.O. Box) Please Print Clearly

Name _____
Institution _____
Street _____
City _____ State _____ Zip _____
Country _____
Quantity_____ Fax _____
Phone: Day _____ Evening _____
E-mail Address _____

Additional Shipping Address* (cannot ship to a P.O. Box)

Name _____
Institution _____
Street _____
City _____ State _____ Zip _____
Country _____
Quantity _____ Fax _____
Phone: Day _____ Evening _____
E-mail Address _____

** Add $32 for each additional shipping address*

Payment and Credit Card Details

Enclosed: Personal Check _____
Credit Card Payment Details _____
Checks must be paid in U.S. dollars and drawn on a U.S. Bank.

Credit Card: __ VISA __ Am. Exp. __ MasterCard
Card Number _____
Expiration Date_____
Signature: _____

Please send your order form and prepayment made payable to:

Cadmus Reprints
P.O. Box 751903
Charlotte, NC 28275-1903

Note: Do not send express packages to this location, PO Box.
FEIN #:541274108

Invoice or Credit Card Information

Invoice Address Please Print Clearly
Please complete Invoice address as it appears on credit card statement

Name _____
Institution _____
Department _____
Street _____
City _____ State _____ Zip _____
Country _____
Phone _____ Fax _____
E-mail Address _____

Cadmus will process credit cards and *Cadmus Journal Services* will appear on the credit card statement.

If you don't mail your order form, you may fax it to 410-820-9765 with your credit card information.

Signature _____ Date _____
Signature is required. By signing this form, the author agrees to accept the responsibility for the payment of reprints and/or all charges described in this document.

RB-9/22/06

Radiology 2007

Black and White Reprint Prices

Domestic (USA only)						
# of Pages	50	100	200	300	400	500
1-4	$213	$228	$260	$278	$295	$313
5-8	$338	$373	$420	$453	$495	$530
9-12	$450	$500	$575	$635	$693	$755
13-16	$555	$623	$728	$805	$888	$965
17-20	$673	$753	$883	$990	$1,085	$1,185
21-24	$785	$880	$1,040	$1,165	$1,285	$1,413
25-28	$895	$1,010	$1,208	$1,350	$1,498	$1,638
29-32	$1,008	$1,143	$1,363	$1,525	$1,698	$1,865
Covers	$95	$118	$218	$320	$428	$530

International (includes Canada and Mexico)						
# of Pages	50	100	200	300	400	500
1-4	$263	$275	$330	$385	$430	$485
5-8	$415	$443	$555	$650	$753	$850
9-12	$563	$608	$773	$930	$1,070	$1,228
13-16	$698	$760	$988	$1,185	$1,388	$1,585
17-20	$848	$925	$1,203	$1,463	$1,705	$1,950
21-24	$985	$1,080	$1,420	$1,725	$2,025	$2,325
25-28	$1,135	$1,248	$1,640	$1,990	$2,350	$2,698
29-32	$1,273	$1,403	$1,863	$2,265	$2,673	$3,075
Covers	$148	$168	$308	$463	$615	$768

Minimum order is 50 copies. For orders larger than 500 copies, please consult Cadmus Reprints at 800-407-9190.

Reprint Cover

Cover prices are listed above. The cover will include the publication title, article title, and author name in black.

Shipping

Shipping costs are included in the reprint prices. Domestic orders are shipped via UPS Ground service. Foreign orders are shipped via a proof of delivery air service.

Multiple Shipments

Orders can be shipped to more than one location. Please be aware that it will cost $32 for each additional location.

Delivery

Your order will be shipped within 2 weeks of the journal print date. Allow extra time for delivery.

Color Reprint Prices

Domestic (USA only)						
# of Pages	50	100	200	300	400	500
1-4	$218	$233	$343	$460	$579	$697
5-8	$343	$388	$584	$825	$1,069	$1,311
9-12	$471	$503	$828	$1,196	$1,563	$1,935
13-16	$601	$633	$1,073	$1,562	$2,058	$2,547
17-20	$738	$767	$1,319	$1,940	$2,550	$3,164
21-24	$872	$899	$1,564	$2,308	$3,045	$3,790
25-28	$1,004	$1,035	$1,820	$2,678	$3,545	$4,403
29-32	$1,140	$1,173	$2,063	$3,048	$4,040	$5,028
Covers	$95	$118	$218	$320	$428	$530

International (includes Canada and Mexico))						
# of Pages	50	100	200	300	400	500
1-4	$268	$280	$412	$568	$715	$871
5-8	$419	$457	$720	$1,022	$1,328	$1,633
9-12	$583	$610	$1,025	$1,492	$1,941	$2,407
13-16	$742	$770	$1,333	$1,943	$2,556	$3,167
17-20	$913	$941	$1,641	$2,412	$3,169	$3,929
21-24	$1,072	$1,100	$1,946	$2,867	$3,785	$4,703
25-28	$1,246	$1,274	$2,254	$3,318	$4,398	$5,463
29-32	$1,405	$1,433	$2,561	$3,788	$5,014	$6,237
Covers	$148	$168	$308	$463	$615	$768

Tax Due

Residents of Virginia, Maryland, Pennsylvania, and the District of Columbia are required to add the appropriate sales tax to each reprint order. For orders shipped to Canada, please add 7% Canadian GST unless exemption is claimed.

Ordering

Reprint order forms and purchase order or prepayment is required to process your order. Please reference journal name and reprint number or manuscript number on any correspondence. You may use the reverse side of this form as a proforma invoice. Please return your order form and prepayment to:

Cadmus Reprints
P.O. Box 751903
Charlotte, NC 28275-1903

Note: Do not send express packages to this location, PO Box.
FEIN #:541274108

Please direct all inquiries to:

Rose A. Baynard
800-407-9190 (toll free number)
410-819-3966 (direct number)
410-820-9765 (FAX number)
baynardr@cadmus.com (e-mail)

Reprint Order Forms and purchase order or prepayments must be received 72 hours after receipt of form.